Journal of Molecular Graphics and Modelling 50 (2014) 90–99

Contents lists available at ScienceDirect

Journal of Molecular Graphics and Modelling

journal homepage: www.elsevier.com/locate/JMGM

Theoretical investigation on gas-phase reaction of $CF_3CH_2OCH_3$ with OH radicals and fate of alkoxy radicals ($CF_3CH(O^•)OCH_3$/$CF_3CH_2OCH_2O^•$)

Bhupesh Kumar Mishra [a], Makroni Lily [b], Ramesh Chandra Deka [a,*], Asit K. Chandra [b,**]

[a] Department of Chemical Sciences, Tezpur University, Tezpur, Assam 784028, India
[b] Department of Chemistry, North-Eastern Hill University, Shillong 793022, India

ARTICLE INFO

Article history:
Accepted 27 March 2014
Available online 5 April 2014

Keywords:
Hydrofluoroether
Isodesmic reactions
Rate constant
Atmospheric lifetime
Alkoxy radical

ABSTRACT

Detailed theoretical investigation has been performed on the mechanism, kinetics and thermochemistry of the gas phase reactions of $CF_3CH_2OCH_3$ (HFE-263fb2) with OH radicals using *ab-initio* and DFT methods. Reaction profiles are modeled including the formation of pre-reactive and post-reactive complexes at entrance and exit channels, respectively. Our calculations reveal that hydrogen abstraction from the $—CH_2$ group is thermodynamically and kinetically more facile than that from the $—CH_3$ group. Using group-balanced isodesmic reactions, the standard enthalpies of formation for $CF_3CH_2OCH_3$ and radicals (CF_3CHOCH_3 and $CF_3CH_2OCH_2$) are also reported for the first time. The calculated bond dissociation energies for the C—H bonds are in good agreement with experimental results. At 298 K, the calculated total rate coefficient for $CF_3CH_2OCH_3$ + OH reactions is found to be in good agreement with the experimental results. The atmospheric fate of the alkoxy radicals, $CF_3CH(O^•)OCH_3$ and $CF_3CH_2OCH_2O^•$ are also investigated for the first time using the same level of theory. Out of three plausible decomposition channels, our results clearly point out that reaction with O_2 is not the dominant path leading to the formation of $CF_3C(O)OCH_3$ for the decomposition of $CF_3CH(O)OCH_3$ radical in the atmosphere. This is in accord with the recent report of Osterstrom et al. [CPL 524 (2012) 32] but found to be in contradiction with experimental finding of Oyaro et al. [JPCA 109 (2005) 337].

© 2014 Elsevier Inc. All rights reserved.

1. Introduction

Volatile organic compounds like hydrofluoroethers (HFEs) are designed and widely recommended as a third generation replacement for chlorofluocarbons (CFCs), hydrofluorocarbons (HFCs) and hydrochlorofluorocarbons (HCFCs) in applications such as cleaning of electronic equipments, heat transfer fluid in refrigerators, lubricant deposition and foam blowing agents [1,2]. Hydrofluoroethers do not contain chlorine and bromine atoms that cause the ozone depletion [3]. In addition, the rate constant for the reaction of HFEs with OH radical suggest that their atmospheric lifetime should be relatively short and thus HFEs appear to have less impact for the global warming [4]. Like most volatile organic compounds, HFEs containing C—H bonds are removed from the troposphere by reactions with atmospheric oxidants, OH radicals being the most dominant oxidant. The tropospheric oxidation of HFEs is known to produce corresponding hydrofluorinated esters (FESs) [5–7]. Like HFEs, FESs also undergo photochemical oxidation in troposphere with atmospheric oxidants, OH radicals or Cl atoms in marine environment. The degradation of FESs produce environmentally burdened product like trifluoroacetic acid (TFA) and COF_2. TFA detected in surface waters has no known sink apart from rainwater and this species may impact on agricultural and aquatic systems [8]. Hence it is important to study the kinetics and mechanistic degradation pathways of HFEs in troposphere for complete assessment of its atmospheric chemistry as well as its impact on global warming and climate change. Therefore, much attention has been paid recently on studying the reactivity of OH and Cl-initiated hydrogen abstraction reactions of HFEs [9–17].

In our present work, we have studied the mechanism and kinetics of H-abstraction reactions between $CF_3CH_2OCH_3$ and OH radicals using DFT and *ab-initio* methods. Our calculation suggests

* Corresponding author. Tel.: +91 3712267008; fax: +91 3712267005.
** Corresponding author. Tel.: +91 3642722622; fax: +91 3642550486.
E-mail addresses: ramesh@tezu.ernet.in (R.C. Deka), akchandra@nehu.ac.in (A.K. Chandra).

http://dx.doi.org/10.1016/j.jmgm.2014.03.009
1093-3263/© 2014 Elsevier Inc. All rights reserved.

that one reaction channel from $-CH_2$ and two reaction channels from $-CH_3$ groups are feasible for the $CF_3CH_2OCH_3$ + OH reactions as given below:

$$CF_3CH_2OCH_3 + OH \rightarrow CF_3CHOCH_3 + H_2O \quad (1)$$

$$CF_3CH_2OCH_3 + OH \rightarrow CF_3CH_2OCH_2 + H_2O \quad (2a \text{ and } 2b)$$

The atmospheric and kinetic studies of the title reaction were investigated experimentally by several groups. Zhang et al. [9] used flash photolysis resonance fluorescence (FPRF) technique to measure the rate coefficient of the OH reaction with $CF_3CH_2OCH_3$ at 296 K and reported it to be $(6.24 \pm 0.67) \times 10^{-13}$ cm^3 molecule^{-1} s^{-1}. Oyaro et al. [10] used gas chromatography–mass spectroscopy (GC–MS) detection and reported a rate constants as $k(OH + CF_3CH_2OCH_3) = (5.7 \pm 0.8) \times 10^{-13}$ cm^3 molecule^{-1} s^{-1} at 298 K and 1013 hPa. Kambanis et al. [11] studied the reactivity of $CF_3CH_2OCH_3$ (HFE-263fb2) with Cl atoms and reported that hydrogen abstraction from methylene group is dominant channel than the methyl group. Recently, Østerstrøm et al. [12] also investigated the atmospheric oxidation mechanism of HFE-263fb2 with OH radicals and Cl atoms using FTIR smog chamber technique and proposed that the major removal process for $CF_3CH_2OCH_3$ in the atmosphere is reaction with OH radicals. They also proposed that hydrogen abstraction by OH radicals proceeds $55 \pm 5\%$ from the $-CH_3$ group and $45 \pm 5\%$ from the $-CH_2$ group. This finding contradicts with the observation of Oyaro et al. [10] that the $-CH_2$ group is more reactive than $-CH_3$ group toward hydrogen abstraction reaction by OH radicals. Recently, Østerstrøm et al. [12] also investigated the atmospheric oxidation mechanism of HFE-263fb2 and proposed that reaction with O_2 is not a competing reaction for $CF_3CH(O)OCH_3$ alkoxy radical which is in contrast with the experimental findings of Oyaro et al. [10] that reaction with O_2 is the dominant loss process for decomposition of $CF_3CH(O)OCH_3$ alkoxy radical. Due to this conflict, there is a desirable need to perform quantum mechanical calculations to determine the energetics involved during the decomposition of $CF_3CH(O)OCH_3$ alkoxy radical. This motivated us to investigate the decomposition reaction mechanism of this radical on a sound theoretical basis. To the best of our knowledge, no theoretical study has been performed to elucidate the dissociative pathways of alkoxy radicals derived from HFE-263fb2. However, experimental studies provided only the total rate constant and it is difficult to predict the detailed mechanism and thermo chemistry. Thus, for better understanding of mechanistic pathways, kinetics and thermochemistry we must rely on quantum chemical methods. The aim of the present paper is to have a more accurate thermo chemical data using modern DFT functional and G2(MP2) method.

The tropospheric degradation of $CF_3CH_2OCH_3$ is initiated by attack of Cl atoms which leads to the formation of alkyl radical CF_3CHOCH_3. The latter reacts with atmospheric O_2 to produce peroxy radical, $CF_3CH(OO)OCH_3$. In a polluted atmosphere the peroxy radical thus formed may further reacts with other oxidizing species such as NO_2 and NO that ultimately leads to the formation of alkoxy radical $CF_3CH(O)OCH_3$. On the other hand, alkoxy radical, $CF_3CH_2OCH_2O$ may also be generated through hydrogen abstraction from the $-CH_3$ group. The chemistry of alkoxy radicals, thus generated has been a subject of extensive experimental and theoretical investigations as these species are interesting intermediates in the atmospheric oxidation of halogenated hydrocarbons. During the recent past, substantial theoretical studies have been performed on atmospheric fate of similar alkoxy radicals [18–24].

There are three potential pathways for decomposition of alkoxy radicals produced from $CF_3CH_2OCH_3$ that involve bond scissions and oxidation processes. These are represented as follows:

$$CF_3CH(O^\bullet)OCH_3 \rightarrow C^\bullet F_3 + CH_3OC(O)H \quad (3)$$

$$\rightarrow CF_3C(O)OCH_3 + H \quad (4)$$

$$+O_2 \rightarrow CF_3C(O)OCH_3 + HO^\bullet{}_2 \quad (5)$$

$$CF_3CH_2OCH_2O^\bullet \rightarrow CF_3CH_2O^\bullet + CH_2O^\bullet \quad (6)$$

$$+O_2 \rightarrow CF_3CH_2OCHO + HO^\bullet{}_2 \quad (7)$$

$$\rightarrow CF_3CH_2OCHO + H \quad (8)$$

Using the power of quantum chemistry methods, here our purpose is twofold: (i) gaining some insight into the fate of the alkoxy radicals, for analyzing the mechanism of the assumed oxidation with O_2 which leads to the formation of $CF_3C(O)OCH_3$ and $HO^\bullet{}_2$, and, (ii) studying the importance of the other pathways that these radicals may undergo.

2. Computational methods

Geometry optimization of the reactants, products and transition states were made at the MPWB1K [25] level of theory using 6-31+G(d,p) basis set. Previous works have shown that the MPWB1K hybrid density functional provides reliable results for thermochemistry and kinetics [26–29]. In order to determine the nature of different stationary points on the potential energy surface, vibrational frequencies calculations were performed using the same level of theory at which the optimization was made. All the stationary points had been identified to correspond to stable minima by ascertaining that all the vibrational frequencies had real positive values. The transition states were characterized by the presence of only one imaginary frequency. To ascertain that the identified transition states connect reactant and product sides smoothly, intrinsic reaction coordinate (IRC) calculations [30] were performed at the MPWB1K/6-31+G(d,p) level. As the reaction energy barriers are very much sensitive to the theoretical levels, the higher-order correlation corrected relative energies along with the density functional energies are necessary to obtain theoretically consistent reaction energies. Therefore, a potentially high-level method such as G2(MP2) [31] has been used for single-point energy calculations. The G2(MP2) [31] energy is calculated in the following manner:

$$E[G2(MP2)] = E_{base} + \Delta E(MP2) + HLC + ZPE$$

where $E_{base} = E$[QCISD(T)/6-311G(d,p)], $\Delta E(MP2) = E$[MP2/6-311 + G(3df,2p)] $- E$[MP2/6-311G(d,p)], HLC (high level correction) $= -0.00481n_\beta - 0.00019n_\alpha$ (n_α and n_β are the number of α and β valence electrons with $n_\alpha \geq n_\beta$) and ZPE = zero-point energy.

In this work the geometry and frequency calculations were performed at MPWB1K/6-31+G(d,p) level. The ZPE thus obtained was corrected with a scale factor of 0.951 to partly eliminate the systematic errors. This dual level calculation (G2(MP2)//MPWB1K) is known to produce reliable kinetic data [27,29,32–37]. All calculations were performed with the Gaussian 09 suite of program [38]. To validate the results obtained at MPWB1K level, we have also optimized species at the M06-2X [39] method using 6-31+G(d,p) basis set.

3. Results and discussion

The calculated enthalpy of reactions ($\Delta_r H^\circ$) and reaction free energies ($\Delta_r G^\circ$) at 298 K for the reaction of $CF_3CH_2OCH_3$ with OH radicals are recorded in Table 1. Free energy values show that both reactions are exergonic ($\Delta G < 0$). The reaction enthalpy ($\Delta_r H^\circ$) values for reactions (1) and (2a and 2b) clearly show that both reactions are exothermic in nature. The results given in Table 1 reveal that both the reaction channels are thermodynamically facile, but hydrogen abstraction from the $-CH_2$ group is more exothermic than that from the $-CH_3$ group.

Table 1
Reaction enthalpies and free energies of reactions (1) and (2a and 2b) calculated at various level of theories. All values are in kcal mol^{-1}.

Reaction channels	ΔH°_{298}			ΔG°_{298}		
	MPWB1K	M06-2X	G2(MP2)	MPWB1K	M06-2X	G2(MP2)
1	−20.21	−20.74	−22.02	−21.79	−23.35	−23.60
2	−17.78	−18.61	−20.87	−18.99	−19.54	−22.08

There are two potential hydrogen abstraction sites of $CF_3CH_2OCH_3$, namely the $-CH_2$ and $-CH_3$ group. However, as can be seen from the geometrical parameters and stereographical orientation, the hydrogen atoms in the $-CH_3$ group are not equivalent. One H-atom (C1—H4) is different from the other two (C1—H3 and C1—H5) in the $-CH_3$ group as shown in Fig. 1. Three transition states (TSs) are therefore, located for $CF_3CH_2OCH_3$ + OH reactions; one TS for H-abstraction from the $-CH_2$ group (TS1) and two TSs

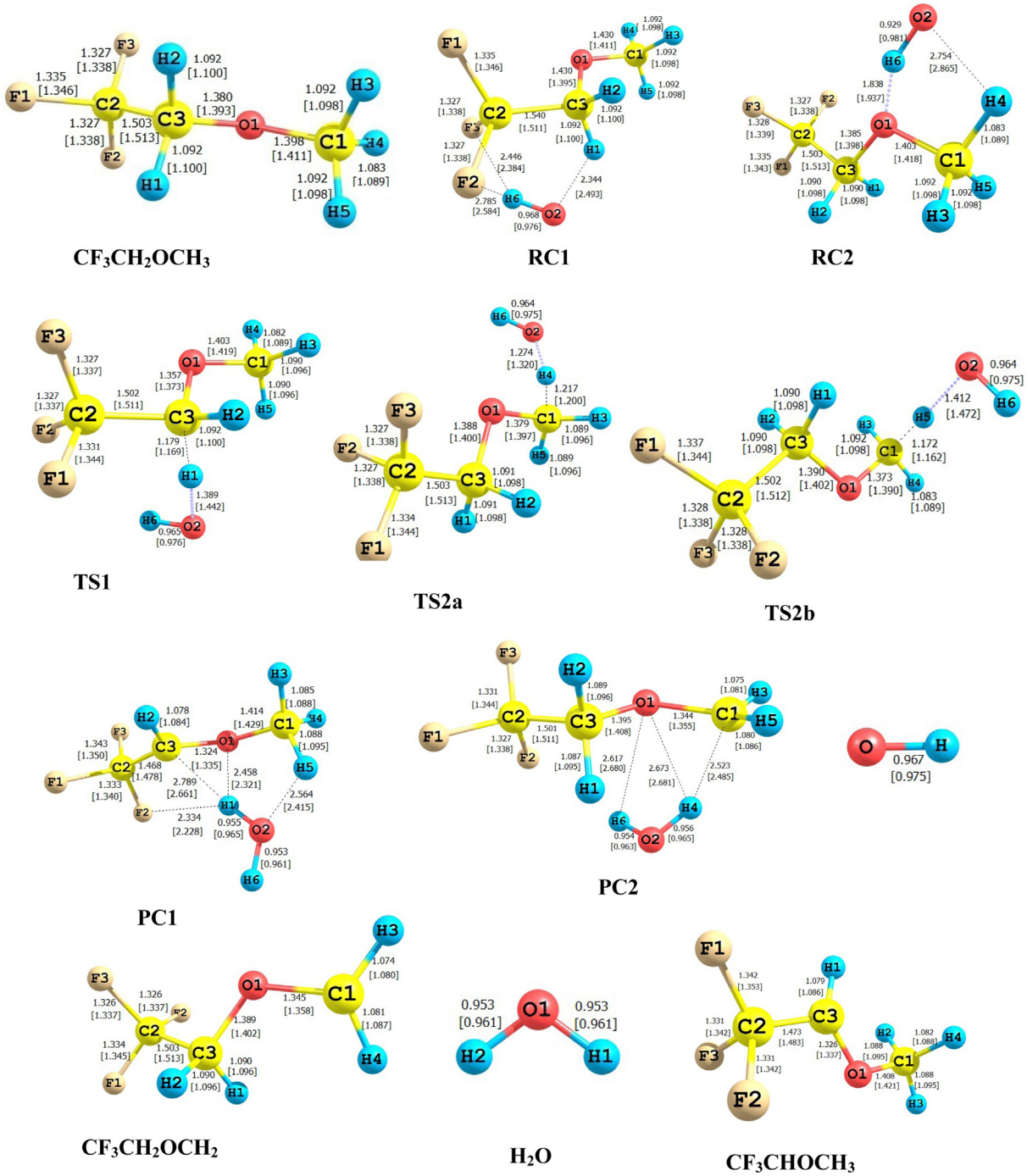

Fig. 1. Optimized geometries of reactants, reactant complexes, transition states, product complexes and products involved in the H atom abstraction reactions of $CF_3CH_2OCH_3$ by OH radicals at MPWB1K and M06-2X (values are given in brackets) levels. Bond lengths are in Angstroms.

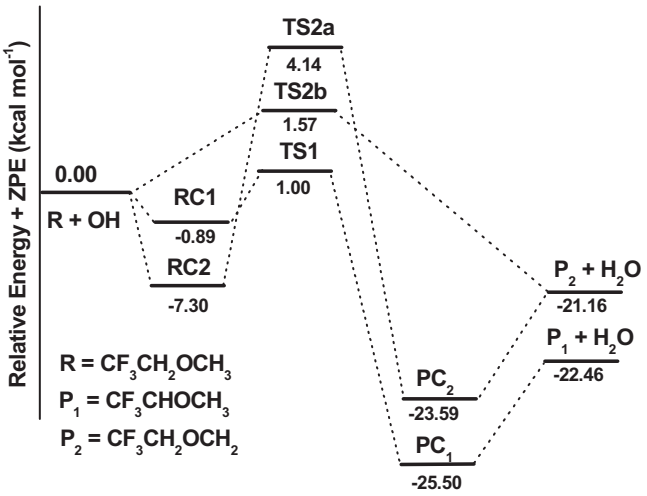

Fig. 2. Schematic potential energy diagram for the $CF_3CH_2OCH_3$ + OH reactions. Relative energies (in kcal mol^{-1}) with ZPE correction at G2(MP2) method.

for the same from the —CH_3 group (TS2a and TS2b). Therefore three H-abstraction reaction channels exist for the reactions studied here. Optimized geometries of reactant, reactant complexes, transition states, product complexes and products obtained at the MPWB1K/6-31+G(d,p) level are shown in Fig. 1. Structures of these species are also optimized at M06-2X/6-31+G(d,p) level of theory and corresponding results are shown in the same figure for comparison. As shown in Fig. 1 the geometrical parameters obtained at two levels of theory are reasonably in good agreement with each other. We could also locate hydrogen bonded complexes present on the reactants and products sides of the primary reaction channels, indicating that the reaction between HFE and OH proceeds through the formation of pre- and post-reactive complexes via an indirect mechanism for each reaction channel (as shown in Fig. 2). The optimized structures of the pre-reaction (RC) and post-reaction (PC) complexes were shown in Fig. 1. Two pre-reactive complexes (RC1 and RC2) were located at the entry point of two reaction channels originated from $CF_3CH_2OCH_3$. On other hand, two post-reaction complexes (PC1 and PC2) were found at the exit channels of the reaction. These RC complexes are formed due to weak interaction between $CF_3CH_2OCH_3$ and OH radical through C—H. . .O and OH. . .F/O hydrogen bonding, whereas the two PC complexes are resulted from the hydrogen bonding interaction between $CF_3CH_2OCH_3$ radical and H_2O molecule. The search was made along the minimum energy path on a relaxed potential energy surface. Visualization of the optimized structure of TS1 further reveals the elongation of C—H (C3—H1) bond length from 1.092 to 1.179 Å (8%) at MPWB1K and 1.100 to 1.169 Å (6%) at the M06-2X level, whereas the newly formed H—O bond is increased from 0.953 to 1.389 Å resulting in an increase of about 45% at MPWB1K and 0.961 to 1.442 Å (50%) at the M06-2X level. Similarly, for transition states TS2a and TS2b for reactions (2a and 2b), the length of the breaking C—H bond is found to be longer in a range of 5.8–12.1% than the observed C—H bond length in isolated $CF_3CH_2OCH_3$; whereas the forming O. . .H bond length is longer by 33–53% than the O—H bond length in H_2O. The fact that the elongation of forming bond is larger than that of the breaking bond indicates that the barrier of the reactions (1) and (2a and 2b) is near the corresponding reactants. This means the reaction will precede via early transition state structure which is in consonance with Hammond's postulate [40] applied to an exothermic hydrogen abstraction reaction.

Results obtained by frequency calculations for species involved in reactions (1) and (2a and 2b) are recorded in Table S1 in Supporting information. These results show that the reactants and products have stable minima on their potential energy surface characterized by the occurrence of only real positive vibrational frequencies. On the other hand, transition states are characterized by the occurrence of only one imaginary frequency obtained at 749i, 1478i and 626i cm^{-1} at the MPWB1K/6-31+G(d,p) and 932i, 1311i and 821i cm^{-1} at the M06-2X/6-31+G(d,p) for TS1, TS2a and TS2b, respectively. Visualization of the normal-mode corresponding to the calculated imaginary frequencies shows a well-defined transition state geometry connecting reactants and products during transition. The existence of transition state on the potential energy surface is further ascertained by intrinsic reaction coordinate (IRC) calculation [30] performed at the same level of theory using the Gonzalez–Schlegel steepest descent path in the mass-weighted Cartesian coordinates with a step size of 0.01(amu$^{1/2}$-bohr).

Single point energy calculations of various species involved in the hydrogen abstraction reactions were performed at the G2(MP2) level using the MPWB1K/6-31+G(d,p) optimized geometries. The associated energy barriers corresponding to reactions (1) and (2a and 2b) calculated from the results obtained at the two above-mentioned theoretical levels are recorded in Table S2 in Supporting information. These results show that energy barriers for H atom abstraction by OH radicals from the —CH_2 group of $CF_3CH_2OCH_3$ are 1.00 kcal mol^{-1} and 0.54 kcal mol^{-1} at the G2(MP2) and the MPWB1K/6-31G + (d,p) level of theory, respectively. On the other hand, the same from the —CH_3 group are found to be 4.14 kcal mol^{-1} and 1.57 kcal mol^{-1} for reactions (2a and 2b), respectively, at the G2(MP2) and 3.25 kcal mol^{-1} and 1.20 kcal mol^{-1}, respectively at the MPWB1K level. The barrier height values show that hydrogen abstraction by OH radicals from the —CH_2 group of $CF_3CH_2OCH_3$ is more facile than that from the —CH_3 group. This finding is in line with the experimental observation by Oyaro et al. [10] and Kambanis et al. [11] as well as to the fact that the calculated C—H bond dissociation energy from —CH_2 group (96.09 kcal mol^{-1}) is lower than that for the —CH_3 group (97.45 kcal mol^{-1}). However, this finding contradicts with the observation of Østerstrøm et al. [12] that hydrogen abstraction by OH radicals proceeds 55 ± 5% from the —CH_3 group and 45 ± 5% from the —CH_2 group. Literature survey reveals that there is no experimental data available for the comparison of the energy barrier for the H-atom abstraction reaction of $CF_3CH_2OCH_3$ by OH radicals. However, In order to ascertain the reliability of the calculated values, we compared our results with the values calculated by Zhang et al. [13] for the Cl-initiated hydrogen abstraction reactions from —CH_2 and —CH_3 sites in $CF_3CH_2OCH_3$. The optimized geometries of two transition states are shown in Fig. S1 in Supporting information. Our calculated barrier heights amount to be −4.09 kcal mol^{-1} and −5.46 kcal mol^{-1}, respectively at the G2(MP2)//MPWB1K/6-31G + (d,p) level of theory for the —CH_2 and —CH_3 sites in $CF_3CH_2OCH_3$ + Cl reactions; whereas the same obtained from the MPWB1K calculations amount to be −4.14 kcal mol^{-1} and −5.58 kcal mol^{-1}. Thus, our calculated barrier heights at both levels are in excellent agreement with the reported values of −4.32 and −5.58 kcal mol^{-1} at MC-QCISD//MP2/6-31+G(d,p) level of theory by Zhang et al. [13] Thus, the calculated energy barriers for the title reactions studied here at the G2(MP2)//MPWB1K/6-31+G(d,p) method can be relied upon. This gives us confidence that the energy barriers calculated using the G2(MP2) method on the geometries optimized at the MPWB1K/6-31+G(d,p) level are reliable values for the hydrogen abstraction channels considered in the present study. A potential energy diagram of the title reactions is constructed with the results obtained at the G2(MP2)//MPWB1K/6-31+G(d,p) level and is shown in Fig. 2. In the construction of energy diagram zero-point corrected total energy data as recorded in Table S2 in Supporting information are utilized and the sum of the zero point corrected ground state energies of $CF_3CH_2OCH_3$ and

OH radical is arbitrarily taken as zero. The pre-reactive complexes (RC1 and RC2) lie below the corresponding reactants by 0.89 and 7.30 kcal mol^{-1}, whereas and post-reactive complexes (PC1 and PC2) are stabilized by 3.04 and 2.43 kcal mol^{-1} at the G2(MP2) level. The barrier heights of the hydrogen abstraction from the $-CH_2$ and $-CH_3$ sites in $CF_3CH_2OCH_3$ by OH radicals are found to be 1.00 kcal mol^{-1}, 4.14 kcal mol^{-1} and 1.57 kcal mol^{-1}, respectively, higher than the corresponding sites in a similar species $CH_3CH_2OCH_3$ and $CF_3CH_2OCHF_2$ [16]. This is in line of the fact that fluorine atom substitution reduces the reactivity of the C—H bonds toward hydrogen abstraction.

The standard enthalpy of formation ($\Delta_fH^\circ_{298}$) at 298 K for $CF_3CH_2OCH_3$ and the radicals generated from hydrogen abstraction, CF_3CHOCH_3 and $CF_3CH_2OCH_2$ can be valuable information for understanding the mechanism and thermochemical properties of their reactions and most importantly for atmospheric modeling, but these values are not yet reported. The group-balanced isodesmic reactions, in which the number and types of bonds are conserved, are used as working chemical reactions herein to calculate the $\Delta_fH^\circ_{298}$. Here, three isodesmic reactions are used to estimate the enthalpies of formation of the species. The used isodesmic reactions are as follows:

a. For $CF_3CH_2OCH_3$

$$CF_3CH_2OCH_3 + CH_4 \rightarrow CH_3OCH_3 + CH_3CF_3 \quad (9)$$

$$CF_3CH_2OCH_3 + CH_2F_2 \rightarrow CF_3OCHF_2 + CH_3CH_3 \quad (10)$$

$$CF_3CH_2OCH_3 + CHF_3 \rightarrow CH_3OCH_3 + CF_3CF_3 \quad (11)$$

b. For CF_3CHOCH_3

$$CF_3CHOCH_3 + CH_4 \rightarrow CF_3CH_2OCH_3 + CH_3 \quad (12)$$

$$CF_3CHOCH_3 + CF_2Cl_2 \rightarrow CF_3OCHF_2 + CH_3CCl_2 \quad (13)$$

$$CF_3CHOCH_3 + CH_2FCl \rightarrow CH_3OCH_3 + CF_3CFCl \quad (14)$$

c. For $CF_3CH_2OCH_2$

$$CF_3CH_2OCH_2 + CH_4 \rightarrow CF_3CH_2OCH_3 + CH_3 \quad (15)$$

$$CF_3CH_2OCH_2 + CHF_2Cl \rightarrow CF_3OCHF_2 + CH_3CHCl \quad (16)$$

$$CF_3CH_2OCH_2 + CH_3Cl \rightarrow CH_3OCH_3 + CF_3CHCl \quad (17)$$

The geometrical parameters of the species involved in isodesmic reactions (9)–(17) were first optimized at the MPWB1K/6-31+G(d,p) level and then energies of the species were further refined at the sophisticated G2(MP2) level of theory. At first we have calculated the reaction enthalpies ($\Delta_rH^\circ_{298}$) of the isodesmic reactions (9)–(17) as mentioned above using total energies of the species obtained at G2(MP2) level including thermal correction to enthalpy estimated at MPWB1K/6-31+G(d,p) level. Since, the ($\Delta_rH^\circ_{298}$) value corresponds to the difference of the enthalpy of formation ($\Delta_fH^\circ_{298}$) values between the products and the reactants, the ($\Delta_fH^\circ_{298}$) values of the reactant and product species are easily evaluated by combining them with the known enthalpies of formation of the reference compounds involved in our isodesmic reaction schemes. The experimental $\Delta_fH^\circ_{298}$ values for CH_4: −17.91 kcal mol^{-1}, CH_3OCH_3: −44.0 kcal mol^{-1}, CH_3CF_3: −179.1 kcal mol^{-1}, CH_3CH_3: −20.01 kcal mol^{-1}, CF_3OCHF_2: −312.30 kcal mol^{-1} and CH_3: 34.85 kcal mol^{-1} are taken from Ref. [41], CH_2F_2: −107.77 kcal mol^{-1}, CHF_3: −166.24 kcal mol^{-1}, CF_2Cl_2: −117.72 kcal mol^{-1}, CH_3Cl: −19.76 kcal mol^{-1}, CH_2Cl_2: −22.41 kcal mol^{-1}, CHF_2Cl: −115.35 kcal mol^{-1} and CH_2FCl: −63.13 kcal mol^{-1} are taken from Ref. [42], CF_3CF_3: −321.20 kcal mol^{-1} [43], CF_3CHCl: −131.93 kcal mol^{-1} [44], CF_3CFCl: −173.41 kcal mol^{-1} [45], CH_3CCl_2: 10.16 kcal mol^{-1} [46] and CH_3CHCl: 18.30 kcal mol^{-1} [46] to evaluate the required enthalpies of formation.

The calculated values of enthalpies of formation are listed in Table 2. As can be seen from Table 2, the values of $\Delta_fH^\circ_{298}$ for the species obtained by the three working chemical reactions are reasonably consistent with each other. The $\Delta_fH^\circ_{298}$ for $CF_3CH_2OCH_3$, CF_3CHOCH_3 and $CF_3CH_2OCH_2$ species calculated from the G2(MP2) results are −205.91 kcal mol^{-1}, −161.96 kcal mol^{-1} and −160.60 kcal mol^{-1}, respectively. Although no comparison between theory and experiment can be made due to the lack of any experimental result, the heat of formation ($\Delta_fH^\circ_{298}$) values can be expected to provide good reference information for upcoming laboratory investigations on thermochemical and kinetic modeling of reactions involving these species, because G2(MP2) method is known to produce reliable thermochemical data.

Table 3 lists the calculated bond-dissociation energies, BDE (D^0_{298}) of the C—H bonds of $CF_3CH_2OCH_3$ molecule along with some experimental data. The D^0_{298} value obtained from the G2(MP2) results for the C—H bonds in the $-CH_2$ and $-CH_3$ sites of $CF_3CH_2OCH_3$ amount to 96.09 kcal mol^{-1} and 97.45 kcal mol^{-1}, respectively. These values for D^0_{298} conform well to the experimental findings of Oyaro et al. [10] for the C—H bond energies at two different carbon center [$CF_3CH(-H)OCH_3$ (95.12 kcal mol^{-1})] and [$CF_3CH_2OCH_2(-H)$ (97.03 kcal mol^{-1})] of $CF_3CH_2OCH_3$. Moreover, our calculated BDE values for the C—H bonds is found to be in good agreement also with the theoretical value of 95.09 kcal mol^{-1} and 97.15 kcal mol^{-1}, respectively for the $-CH_2$ and $-CH_3$ sites of $CF_3CH_2OCH_3$ by Urata et al. [14] and 95.29 and 96.95 kcal mol^{-1} by Zhang et al. [13]. Thus, owing to the lower C—H bond dissociation energy, $-CH_2$ group is more reactive toward hydrogen abstraction than $-CH_3$ group. This is reflected in the calculated barrier height for hydrogen abstraction from $-CH_2$ and $-CH_3$ groups. Similar conclusions are also observed for $CH_3CH_2OCH_3$ and $CF_3CH_2OCHF_2$ species for that $-CH_2$ group is found to be more reactive toward hydrogen abstraction by OH radicals [16].

3.1. Fate of alkoxy radicals

The degradation and thermal decomposition of alkoxy radicals, $CF_3CH(O^\bullet)OCH_3$ and $CF_3CH_2OCH_2O^\bullet$ in the atmosphere is envisaged to occur via reactions (3)–(8). Optimized geometries of radicals and transition states involved in these reactions obtained at the MPWB1K/6-31+G(d,p) level are shown in Fig. 3. The structures of these species are also optimized at the M06-2X/6-31+G(d,p) level of theory and the corresponding results are shown in the same figure for comparison. As shown in Fig. 3, the optimized geometrical parameters obtained at two levels of theory are reasonably in good agreement with each other. Transition states obtained on the potential energy surfaces of reactions (3)–(8) are characterized as TS3, TS4, TS5, TS6, TS7 and TS8, respectively. The search was made along the minimum energy path on a relaxed potential energy surface. Harmonic vibrational frequencies of the stationary points were calculated and are given in Table S3 in Supporting information. These results show that the reactant and products have stable minima on their potential energy surface characterized by the occurrence of only real and positive vibrational frequencies. On the other hand, transition states are characterized by the occurrence of only one imaginary frequency obtained at 447i cm^{-1}, 488i cm^{-1}, 1099i cm^{-1}, 649i cm^{-1} and 871i cm^{-1} at the MPWB1K/6-31+G(d,p) and 398i cm^{-1}, 1260i cm^{-1}, 1014i cm^{-1}, 565i cm^{-1} and 1597i cm^{-1} at the M06-2X/6-31+G(d,p) for TS3, TS4, TS5, TS6, TS7 and TS8, respectively. The existence of these transition states on the potential energy surface is further ascertained by intrinsic IRC calculation [30] performed at the same level of theory. The associated energy barriers corresponding to reactions (3)–(8) calculated at various

Table 2
Enthalpies of formation ($\Delta_f H^\circ_{298}$) (in kcal mol^{-1}) at 298 K from the isodesmic reactions.

Species	Isodesmic reaction schemes	MPWB1K/6-31+G(d,p)	G2(MP2)	M06-2X/6-31+G(d,p)
$CF_3CH_2OCH_3$	9	−204.53	−205.65	−204.85
	10	−204.69	−205.96	−205.27
	11	−206.91	−206.13	−204.91
	Average	−205.37	−205.91	−205.01
CF_3CHOCH_3	12	−163.35	−161.31	−161.27
	13	−161.74	−162.82	−163.08
	14	−163.50	−161.59	−163.2
	Average	−162.86	−161.96	−162.52
$CF_3CH_2OCH_2$	15	−160.92	−160.15	−159.15
	16	−158.77	−160.67	−159.88
	17	−161.29	−160.98	−161.63
	Average	−160.32	−160.60	−160.22

Table 3
Calculated C—H bond dissociation energy (D^0_{298}) along with experimental values. All values are in kcal mol^{-1}.

Bond dissociation type	MPWB1K/6-31+G(d,p)	G2(MP2)	M06-2X/6-31+G(d,p)	Exp. values[a]
C—H bond				
$CF_3CH_2OCH_3 \rightarrow CF_3CHOCH_3 + H$	94.65	96.09	94.63	95.12[a], 92.62[b], 95.09[c], 95.29[d]
$CF_3CH_2OCH_3 \rightarrow CF_3CH_2OCH_2 + H$	97.19	97.45	96.93	97.03[a], 93.31[b], 97.15[c], 96.95[d]

[a] Oyaro et al. [10].
[b] Kambnis et al. [11].
[c] Urata et al. [14].
[d] Zhang et al. [13].

levels of theory are recorded in Table 4. The energy barriers corresponding to reactions (3)–(5) show that the energy barrier for H-abstraction reaction of $CF_3CH(O^\bullet)OCH_3$ radical with molecular O_2 is in the range of 15–18 kcal mol^{-1} depending upon the level of theory used during the calculation whereas it is in the range of 7–9 kcal mol^{-1} for C—C bond scission occurred in its thermal decomposition. Results show that the G2(MP2) method yields a value of 7.97 kcal mol^{-1} and 15.08 kcal mol^{-1} for C—C bond scission and oxidation by molecular O_2, respectively. On the other hand, the MPWB1K method yields corresponding values as 9.22 and 18.0 kcal mol^{-1}. The corresponding energy barriers calculated at M06-2X is found to be 8.72 and 16.41 kcal mol^{-1} as recorded in Table 4. The calculated energy barriers for reactions (3)–(5) from all the three methods clearly show that the C—C bond scission reaction is the dominant reaction pathway and reaction (5) is less important for atmospheric degradation of $CF_3CH(O^\bullet)OCH_3$ radical which is in accord with the conclusion made by Osterstrom et al. [12] but contradict with the experimental finding of Oyaro et al. [10]. Similarly, the energy barriers for H-abstraction reaction of $CF_3CH_2OCH_2O^\bullet$ radical with O_2 is in the range of 8–12 kcal mol^{-1}, whereas it is in the range of 12–17 kcal mol^{-1} and 20–25 kcal mol^{-1} for C—H and C—O bond scissions, respectively depending on the level of theory used. It is obvious from Table 4 that the barrier height (8.53 kcal mol^{-1}) for oxidation of $CF_3CH_2OCH_2O^\bullet$ radical with O_2 is considerably lower than that for other decomposition pathways and the dominance of the oxidative pathways of this alkoxy radical in the atmosphere is thus envisioned. Thus, we conclude that the atmospheric fate of $CF_3CH_2OCH_2O^\bullet$ radical is reaction with O_2 leading to the formation of CF_3CH_2OCHO which is in good agreement with the experimental findings of Oyaro et al. [10] and Østerstrøm et al. [12].

Table 4
Calculated barrier heights (in kcal mol^{-1}) for reactions (3)–(8) at various levels of theory.

Reaction channels	MPWB1K/6-31+G(d,p)	G2(MP2)	M06-2X/6-31+G(d,p)
$CF_3CH(O^\bullet)OCH_3$			
TS3 (C—C bond scission)	9.22	7.97	8.72
TS4 (C—H bond scission)	15.87	12.67	14.35
TS5 (reaction with O_2)	18.00	15.08	16.41
$CF_3CH_2OCH_2O^\bullet$			
TS6 (C—O bond scission)	25.41	20.19	24.31
TS7 (reaction with O_2)	12.64	8.53	10.64
TS8 (C—H bond scission)	17.18	12.08	14.43

3.2. Rate constants

The rate coefficients for hydrogen abstraction reaction were calculated using the canonical transition state theory (TST) [47]:

$$k(T) = s_r G(T) \frac{k_B T}{h} \frac{q_{TS}(T)}{q_{HFE}(T).q_{OH}(T)} e^{-DE_0^{\#}/RT} \quad (18)$$

where $q_x(T)$ represents the partition function for the species x (TS, HFE, OH) at temperature T, k_B is the Boltzmann constant, $\Delta E_0^{\#}$ is the barrier height including ZPE and σ_r is the degeneracy of each reaction channel. The tunneling correction $\Gamma(T)$ was estimated by using the Eckart's unsymmetrical barrier method [48]. All vibrational modes, except for the lowest vibrational mode, were treated quantum mechanically as separable harmonic oscillators, whereas for the lower frequency torsional mode, the partition function was evaluated by the hindered-rotor approximation by Truhlar and Chuang [49] method. Using Truhlar's procedure [50] the q^{HIN}/q^{HO} ratio was estimated and was found to be almost unity. In the calculation of the electronic partition functions, the two electronic states of the OH radicals were included, with a 139.7 cm^{-1} splitting in the $^2\prod$ ground state [51]. The contribution from each of two channels is taken into account while calculating the total rate coefficient (k_{OH}) for the $CF_3CH_2OCH_3$ + OH reactions. The total rate coefficient (k_{OH}) is therefore obtained from the addition of rate coefficients for the two channels: $k_{OH} = k1 + k2a + k2b$. The calculated total rate constant (k_{OH}) values for hydrogen abstraction reactions of $CF_3CH_2OCH_3$ with OH radicals using both MPWB1K and G2(MP2)

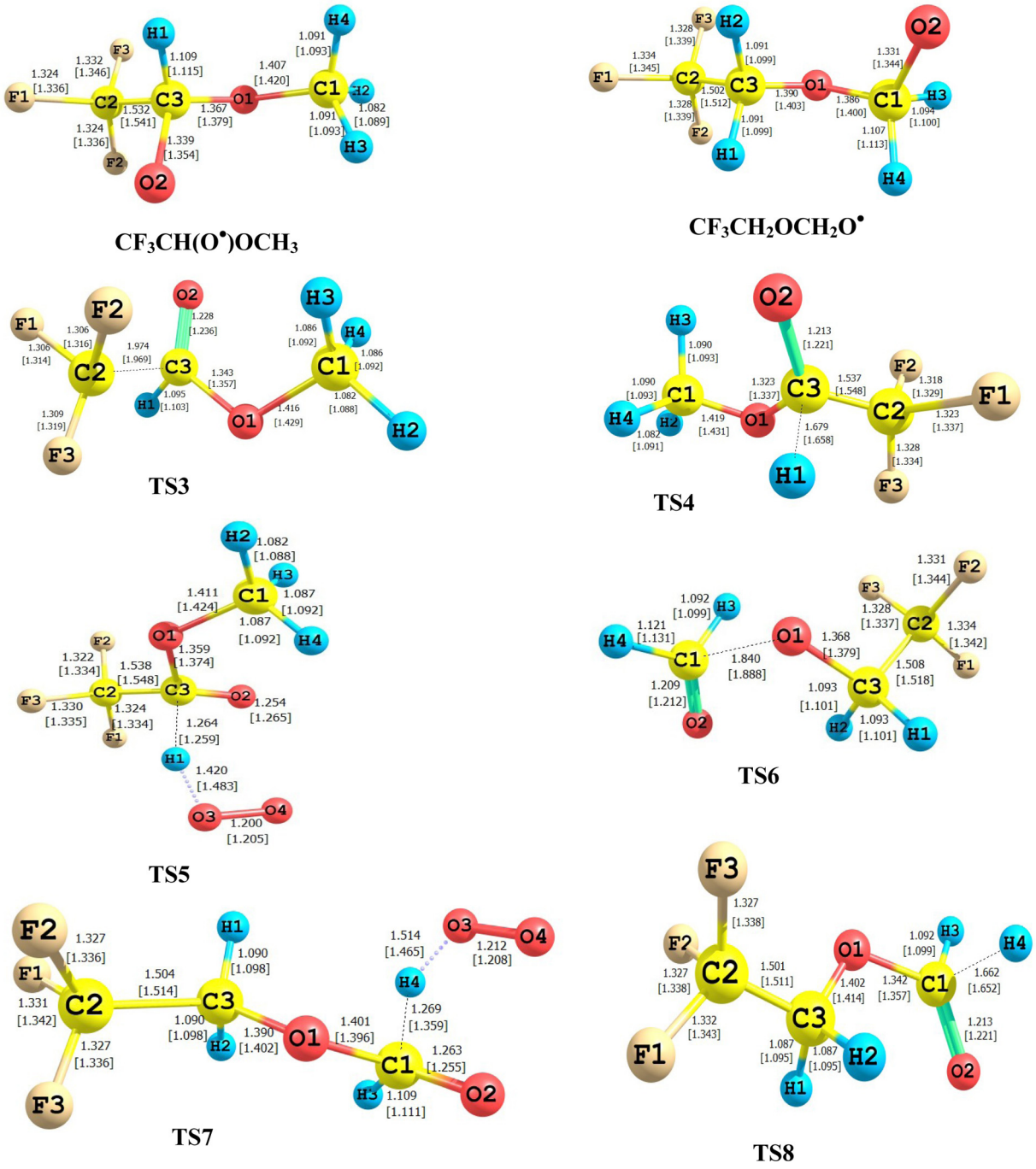

Fig. 3. Optimized geometries of radicals and transition states at MPWB1K and M06-2X (within brackets) levels. Bond lengths are in Angstroms.

barrier heights and within a range of temperature 250–1000 K are presented in Table 5. At 298 K, our calculated k_{OH} value using the MPWB1K barrier heights is 4.68×10^{-13} cm^3 molecule^{-1} s^{-1} which is in very good agreement with the experimental value of $(4.9 \pm 1.3) \times 10^{-13}$ cm^3 molecule^{-1} s^{-1} reported by Østerstrøm et al. [12] and $(5.7 \pm 0.8) \times 10^{-13}$ cm^3 molecule^{-1} s^{-1} by Oyaro et al. [10]. However, the rate coefficient obtained from the G2(MP2) results (2.17×10^{-13} cm^3 molecule^{-1} s^{-1} is somewhat lower but in reasonably good agreement with the MPWB1K and experimental values at 298 K. Temperature variations of k_{OH} results obtained at MPWB1K level along with the experimental results are shown in Fig. 4. Moreover, Our calculated total rate constant using the G2(MP2) and MPWB1K results is found to be higher than the rate constant values for the corresponding hydrofluorocarbon $CF_3CH_2CH_3$ (4.30×10^{-14} cm^3 molecule^{-1} s^{-1}) reported by Gonzalez-Lafont et al. [52]. This suggests that the introduction of ether linkage in hydrofluorocarbons enhance the reactivity of C—H bonds for hydrogen abstraction reactions by OH radicals. Significant non-Arrhenius behavior can be seen from these plots, which is of course expected for multichannel reaction and effect of tunneling.

The temperature variation of the hydrogen abstraction rate constant for this $CF_3CH_2OCH_3$ + OH reactions can be described by a three parameter model equation developed by Zheng and Truhlar [53]

$$k = C \exp\left[-\frac{D_1 - (D_2/T)}{RT}\right] \quad (19)$$

Table 5
Rate constant values (in cm^3 $molecule^{-1}$ s^{-1}) for hydrogen abstraction reactions of $CF_3CH_2OCH_3$ with OH radicals from —CH_2 and —CH_3 groups and total rate constant (k_{OH}) values as calculated using G2(MP2). Total rate constant values obtained from MPWB1K barrier heights are given in last column.

Temp (K)	k_{R1}	k_{R2}	Total rate constant (k_{OH})		Exp. values[a]
			G2(MP2)	MPWB1K	
250.0	0.114E – 12	0.541E – 13	0.168E – 12	0.404E – 12	
298.0	0.143E – 12	0.736E – 13	0.217E – 12	0.468E – 12	0.49E – 12[a], 0.57E – 12[b]
350.0	0.183E – 12	0.108E – 12	0.291E – 12	0.571E – 12	
450.0	0.284E – 12	0.213E – 12	0.497E – 12	0.865E – 12	
550.0	0.420E – 12	0.389E – 12	0.808E – 12	0.130E – 11	
650.0	0.597E – 12	0.663E – 12	0.126E – 11	0.192E – 11	
750.0	0.821E – 12	0.107E – 11	0.189E – 11	0.277E – 11	
850.0	0.110E – 11	0.164E – 11	0.273E – 11	0.389E – 11	
950.0	0.144E – 11	0.241E – 11	0.385E – 11	0.533E – 11	
1000.0	0.163E – 11	0.288E – 11	0.451E – 11	0.618E – 11	

[a] Østerstrøm et al. [12].
[b] Oyaro et al. [10].

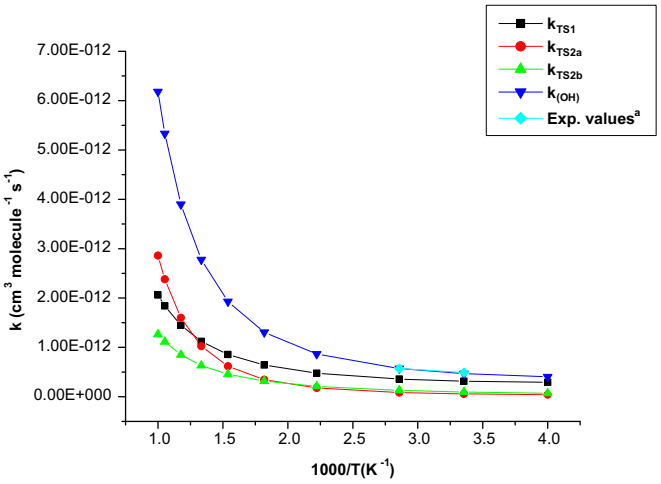

Fig. 4. Rate constants for hydrogen abstraction reactions of $CF_3CH_2OCH_3$ with OH radicals and total rate constant (k_{OH}) for the $CF_3CH_2OCH_3$ + OH reactions.
Source. [a]Ref. [12] (CPL 524 (2012) 32).

where C, D_1 and D_2 are fitting parameters ($D_1 > 0$ and $D_2 > 0$), and R is gas constant. The units of C, D_1 and D_2 in the present case are cm^3 $molecule^{-1}$ s^{-1}, kcal mol^{-1} and K kcal mol^{-1}, respectively.

From above Eq. (19), the activation energy, E_a is given by

$$E_a = \left(D_1 - \frac{2D_2}{T}\right) \quad (20)$$

The G2(MP2) calculated rate constant values for the reaction between $CF_3CH_2OCH_3$ with OH radicals in the temperature range of 250–1000 K is fitted in the model Eq. (19) and found to be well described by the following equations:

$$k_{OH} = 5.25 \times 10^{-11} \exp\left[\frac{-(2970.3 - 389644)/T}{T}\right] \quad (21)$$

The correlation coefficient (R^2) value for the fitting is 0.995 indicating the goodness of this model equation in representing the rate constant values in the said temperature range. The value of activation energy, E_a of $CF_3CH_2OCH_3$ with OH radicals, calculated from Eq. (20) is 0.71 kcal mol^{-1} at 298 K. The rate constant values in this temperature range can be useful for atmospheric modeling calculations that can help to assess the atmospheric lifetimes.

3.3. Atmospheric implications

The atmospheric lifetime of $CF_3CH_2OCH_3$ (τ_{eff}) can be estimated by assuming that its removal from the atmosphere occurs primarily through the reaction with OH radicals. Then τ_{eff} can be expressed as [54]

$$\tau_{eff} \approx \tau_{OH}$$

where $\tau_{OH} = (k_{OH} \times [OH])^{-1}$ and [OH] is the global average OH radical concentration in atmosphere. Taking the global average atmospheric OH radical concentration of 1.0×10^6 molecules cm^{-3} and k_{OH} value at 298 K as 4.68×10^{-13} cm^3 $molecule^{-1}$ s^{-1}, the atmospheric lifetime of $CF_3CH_2OCH_3$ is estimated to be 24 days which is in very good agreement with the experimentally reported atmospheric lifetime of $CF_3CH_2OCH_3$ with respect to the reaction with OH radicals by Hodenbrog et al. [55] (23 days) and Østerstrøm et al. [12] (25 days).

4. Conclusions

The potential energy profile and reaction kinetics of the H atom abstraction reaction of $CF_3CH_2OCH_3$ with OH radicals are investigated at the G2(MP2)//MPWB1K/6-31+G(d,p) level of theory. The reaction is found to follow an indirect path through the formation of pre- and post-reaction complexes. Two important reaction channels have been identified for the reaction. The barrier height for hydrogen abstraction from —CH_2 group calculated at G2(MP2) level are found to be 1.00 kcal mol^{-1}. The thermal rate constant for the H atom abstraction of $CF_3CH_2OCH_3$ by OH radicals is found to be 4.68×10^{-13} cm^3 $molecule^{-1}$ s^{-1} at 298 K using canonical transition state theory which is in very good agreement with experimental data. The temperature variation of rate constant in the range 250–1000 K can be described using model equation as $k_{OH} = 5.25 \times 10^{-11} \exp[(-(2970.3 - 389{,}644)/T)/T]$. From our theoretical study and along with experimental evidence it can be concluded that hydrogen abstraction from methylene group is more facile than that from methyl group. The $\Delta_f H^\circ_{298}$ for $CF_3CH_2OCH_3$, CF_3CHOCH_3 and $CF_3CH_2OCH_2$ species calculated from G2(MP2) results are −205.91 kcal mol^{-1}, −161.96 kcal mol^{-1} and −160.60 kcal mol^{-1}, respectively. The D^0_{298} value obtained from the G2(MP2) results for the C—H bonds in the —CH_2 and —CH_3 sites of $CF_3CH_2OCH_3$ amount to 96.09 kcal mol^{-1} and 97.45 kcal mol^{-1}, respectively. Atmospheric lifetime of $CF_3CH_2OCH_3$ is estimated to be around 24 days. Our results confirm that the reaction with O_2 is not sole atmospheric fate for decomposition of $CF_3CH(O^\bullet)OCH_3$ radical. We hope our theoretical results will help to solve the controversy on —CH_2 versus —CH_3 group contributions to the total rate constant of the title reaction.

Acknowledgments

The authors acknowledge financial support from the Department of Science and Technology, New Delhi in the form of a project (SR/NM.NS-1023/2011(G)). A.K.C. acknowledges CSIR, New Delhi, for financial assistance through project no. 01(2494)/11/EMR-II. B.K.M. is thankful to University Grants Commission, New Delhi (F.4-2/2006(BSR)/13-696/2012(BSR) for providing Dr. D.S. Kothari Post doctoral Fellowship.

Appendix A. Supplementary data

Supplementary data associated with this article can be found, in the online version, at http://dx.doi.org/10.1016/j.jmgm.2014.03.009.

References

[1] M.J. Molina, F.S. Rowland, Stratospheric sink for chlorofluoromethanes: chlorine atom-catalysed destruction of ozone, Nature 249 (1974) 810–812.
[2] A. Sekiya, S. Misaki, The potential of hydrouoroethers to replace CFCs, HCFCs and PFCs, J. Fluorine Chem. 101 (2000) 215–221.
[3] R.L. Powell, CFC phase-out: have we met the challenge? J. Fluorine Chem. 114 (2002) 237–250.
[4] P. Blowers, K.F. Tetrault, Y.T. Morehead, Global warming potential prediction for hydrofluoroethers with two carbon atoms, Theor. Chem. Acc. 119 (2008) 369–381.
[5] M.B. Blanco, I. Bejan, I. Barnes, P. Wiesen, M.A. Teruel, atmospheric photooxidation of fluoroacetates as a source of fluorocarboxylic acids, Environ. Sci. Technol. 44 (7) (2010) 2354–2359.
[6] I. Bravo, Y. Diaz-de-Mera, A. Aranda, M. Elena, D.R. Nutt, G. Marston, Radiative efficiencies for fluorinated esters: indirect global warming potentials of hydrofluoroethers, Phys. Chem. Chem. Phys. 13 (2011) 17185–17193.
[7] Y. Ninomiya, M. Kawasaki, A. Guschin, L.T. Molina, M.J. Molina, T.J. Wallington, Atmospheric chemistry of n-$C_3F_7OCH_3$: reaction with OH radicals and Cl atoms and atmospheric fate of n-$C_3F_7OCH_2O$ radicals, Environ. Sci. Technol. 34 (14) (2000) 2973–2978.
[8] A. Jordan, H. Frank, Trifluoroacetate in the environment. Evidence for sources other than HFC/HCFCs, Environ. Sci. Technol. 33 (4) (1999) 522–527.
[9] Z. Zhang, R.D. Saini, M.J. Kurylo, R.E. Huie, Rate constants for the reactions of the hydroxyl radical with several partially fluorinated ethers, J. Phys. Chem. 96 (1992) 9301–9304.
[10] N. Oyaro, S.R. Sellevig, C.J. Nielsen, Atmospheric chemistry of hydrofluoroethers: reaction of a series of hydrofluoroethers with OH radicals and Cl atoms, atmospheric lifetimes and global warming potentials, J. Phys. Chem. A 109 (2005) 337–346.
[11] K.G. Kambanis, Y.G. Lazarou, P. Papagiannakopoulos, kinetic study for the reactions of chlorine atoms with a series of hydrofluoroethers, J. Phys. Chem. A 102 (1998) 8620–8625.
[12] F.F. Østerstrøm, O.J. Nielsen, M.P.S. Andersen, T.J. Wallington, Atmospheric chemistry of $CF_3CH_2OCH_3$: reaction with chlorine atoms and OH radicals, kinetics, degradation mechanism and global warming potential, Chem. Phys. Lett. 524 (2012) 32–37.
[13] H. Zhang, C.-Y. Liu, G.-L. Zhang, W.-J. Hou, M. Sun, B. Liu, Z.-S. Li, Theoretical studies of the reactions of Cl atoms with $CF_3CH_2OCH_nF_{(3-n)}$ (n = 1, 2, 3), Theor. Chem. Acc. 127 (2010) 551–560.
[14] S. Urata, A. Takada, T. Uchimaru, A.K. Chandra, Rate constants estimation for the reaction of hydrofluorocarbons and hydrofluoroethers with OH radicals, Chem. Phys. Lett. 368 (2003) 215–223.
[15] G. Fontana, M. Causa, V. Gianotti, G. Marchionni, Computational studies of the reaction of the hydroxyl radical with hydrofluorocarbons (HFCs) and hydrofluoroethers (HFEs), J. Fluorine Chem. 109 (2001) 113–121.
[16] L. Yang, J.Y. Liu, L. Wang, H.Q. He, Y. Wang, Z.S. Li, Theoretical study of the reactions $CF_3CH_2OCHF_2$ + OH/Cl and its product radicals and parent ether ($CH_3CH_2OCH_3$) with OH, J. Comp. Chem. 29 (2008) 550–561.
[17] H.J. Singh, B.K. Mishra, Ab-initio studies on the decomposition kinetics of CF_3OCF_2O radical, J. Mol. Model. 17 (2011) 415–422.
[18] E. Henon, F. Bohr, N.S. Gomex, F. Caralp, Degradation of three oxygenated alkoxy radicals of atmospheric interest: $HOCH_2O$, CH_3OCH_2O, $CH_3OCH_2OCH_2O$. RRKM theoretical study of the β-C—H bond scission and the 1,6-isomerisation kinetics, Phys. Chem. Chem. Phys. 5 (2003) 5431–5437.
[19] L. Vereecken, J.S. Francisco, Theoretical studies of atmospheric reaction mechanisms in the troposphere, Chem. Soc. Rev. 41 (2012) 6259–6293.
[20] H.J. Singh, B.K. Mishra, N.K. Gour, Theoretical studies of decomposition kinetics of CF_3CCl_2O radical, Theor. Chem. Acc. 125 (2010) 57–64.
[21] L. Vereecken, J. Peeters, Decomposition of substituted alkoxy radicals. Part I: A generalized structure–activity relationship for reaction barrier heights, Phys. Chem. Chem. Phys. 11 (2009) 9062–9074.
[22] H.J. Singh, B.K. Mishra, P.K. Rao, Computational study on the thermal decomposition and isomerization of the $CH_3OCF_2O^{\bullet}$ radical, Can. J. Chem. 90 (4) (2012) 403–409.
[23] H.J. Singh, B.K. Mishra, Computational study on decomposition kinetics of CH_3CFClO radical, J. Chem. Sci. 123 (2011) 733–741.
[24] H.J. Singh, N.K. Gour, P. Srivastava, Computational studies on the thermal decomposition of the $CH_2FOCHFO$ radical, Mol. Phys. 111 (2013) 3756–3761.
[25] Y. Zhao, D.G. Truhlar, Hybrid meta density functional theory methods for thermochemistry, thermochemical kinetics, and noncovalent interactions: the MPW1B95 and MPWB1K models and comparative assessments for hydrogen bonding and van der Waals interactions, J. Phys. Chem. A 108 (2004) 6908–6918.
[26] Kh.J. Devi, A.K. Chandra, Theoretical investigation of the gas-phase reactions of $(CF_3)_2CHOCH_3$ with OH radical, Chem. Phys. Lett. 502 (2011) 23–28.
[27] H.J. Singh, B.K. Mishra, A computational perspective of the competitive decomposition and isomerization of CH_3OCHFO radical, J. At. Mol. Sci. 4 (3) (2013) 210–224.
[28] T. Zeegers-Huyskens, M. Lily, D. Sutradhar, A.K. Chandra, Theoretical study of the O···Cl interaction in fluorinated dimethyl ethers complexed with a Cl atom: is it through a two-center-three-electron bond? J. Phys. Chem. A 117 (2013) 8010–8016.
[29] A.K. Chakrabartty, B.K. Mishra, D. Bhattacharjee, R.C. Deka, Theoretical study on the kinetics and branching ratios of the gas phase reactions of 4,4,4-trifluorobutanal (TFB) with OH radical in the temperature range of 250–400 K and atmospheric pressure, J. Fluorine Chem. 154 (2013) 60–66.
[30] H.P. Hratchian, H.B. Schlegel, Using Hessian updating to increase the efficiency of a Hessian based predictor-corrector reaction path following method, J. Chem. Theory Comput. 1 (2005) 61–69.
[31] L.A. Curtiss, K. Raghavachari, J.A. Pople, Gaussian-2 theory using reduced Moller–Plesset orders, J. Chem. Phys. 98 (1993) 1293–1298.
[32] B.K. Mishra, M. Lily, A.K. Chakrabartty, R.C. Deka, A.K. Chandra, A DFT study on kinetics of the gas phase reactions of $CH_3CH_2OCF_3$ with OH radicals and Cl atoms, J. Fluorine Chem. 159 (2014) 57–64.
[33] R.C. Deka, B.K. Mishra, A theoretical investigation on the kinetics, mechanism and thermochemistry of gas-phase reactions of methyl acetate with chlorine atoms at 298 K, Chem. Phys. Lett. 595 (2014) 43–47.
[34] M. Lily, D. Sutradhar, A.K. Chandra, Theoretical investigations on kinetics, mechanism and thermochemistry of the gas-phase reactions of $CHF_2OCF_2CHF_2$ with OH radicals, Comput. Theor. Chem. 1022 (2013) 50–58.
[35] B.K. Mishra, A.K. Chakrabartty, R.C. Deka, Theoretical study on rate constants for the reactions of $CF_3CH_2NH_2$ (TFEA) with the hydroxyl radical at 298 K and atmospheric pressure, J. Mol. Model. 19 (2013) 2189–2195.
[36] A.K. Chakrabartty, B.K. Mishra, D. Bhattacharjee, R.C. Deka, Mechanistic and kinetics study of the gas phase reactions of methyltrifluoroacetate with OH radical and Cl atom, Mol. Phys. 111 (2013) 860–867.
[37] A.K. Chandra, Theoretical studies on the kinetics and mechanism of the gas-phase reactions of CHF_2OCHF_2 with OH radicals, J. Mol. Model. 18 (2012) 4239–4247.
[38] M.J. Frisch, G.W. Trucks, H.B. Schlegel, G.E. Scuseria, M.A. Robb, J.R. Cheeseman, G. Scalmani, V. Barone, B. Mennucci, G.A. Petersson, et al., Gaussian 09, Revision B.01, Gaussian, Inc., Wallingford, CT, 2010.
[39] Y. Zhao, D.G. Truhlar, The M06 suite of density functionals for main group thermochemistry, thermochemical kinetics, noncovalent interactions, excited states, and transition elements: two new functionals and systematic testing of four M06-class functionals and 12 other functionals, Theor. Chem. Acc. 120 (2008) 215–241.
[40] G.S. Hammond, A correlation of reaction rates, J. Am. Chem. Soc. 77 (1955) 334–338.
[41] J.Y. Wu, J.Y. Liu, Z.S. Li, C.C. Sun, Theoretical study of the reactions of CF_3OCHF_2 with the hydroxyl radical and the chlorine atom, ChemPhysChem 5 (2004) 1336–1344.
[42] J. Csontos, Z. Rolik, S. Das, M. Kallay, High-accuracy thermochemistry of atmospherically important fluorinated and chlorinated methane derivatives, J. Phys. Chem. A 114 (2010) 13093–13103.
[43] S.S. Chen, A.S. Rodgers, J. Chao, R.C. Wilhoit, B.J. Zwolinski, Ideal gas thermodynamic properties of six fluoroethanes, J. Phys. Chem. Ref. Data 4 (1975) 441–456.
[44] L. Wang, Y. Zhao, J. Zhang, Y. Dai, J. Zhang, Dual-level direct dynamics studies on the hydrogen abstraction reactions of fluorine atoms with CF_3CH_2X (X = F, Cl), Theor. Chem. Acc. 128 (2011) 183–189.
[45] B. Li, J.Y. Liu, Z.S. Li, J.Y. Wu, C.C. Sun, Theoretical studies on dynamics and thermochemistry of the reactions $CF_3CHCl_2 + Cl \rightarrow CF_3CCl_2 + HCl$ and $CF_3CHFCl + Cl \rightarrow CF_3CFCl + HCl$, J. Chem. Phys. 120 (2004) 6019.
[46] J.A. Seetula, Kinetics and thermochemistry of the R + HBrJ⇔JRH + Br (R = CH_2Cl, $CHCl_2$, CH_3CHCl or CH_3CCl_2) equilibrium, J. Chem. Soc. Faraday Trans. 92 (1996) 3069–3078.
[47] K.J. Laidler, Chemical Kinetics, third ed., Pearson Education, Delhi, 2004.
[48] H.S. Johnston, J. Heicklen, Tunnelling corrections for unsymmetrical Eckart potential energy barriers, J. Phys. Chem. 66 (1962) 532–533.
[49] Y.Y. Chuang, D.G. Truhlar, Statistical thermodynamics of bond torsional modes, J. Chem. Phys. 112 (2000) 1221–1228.
[50] D.G. Truhlar, A simple approximation for the vibrational partition function of a hindered internal rotation, J. Comput. Chem. 12 (1991) 266–270.

[51] M.W. Chase Jr., NIST-JANAF Thermochemical Tables, J. Phys. Chem. Ref. Data, fourth ed., 1998, pp. 1 (Monograph No. 9).
[52] A. Gonzalez-Lafont, J.M. Lluch, A. Varela-Alvarez, J.A. Sordo, Canonical variational transition-state theory study of the $CF_3CH_2CH_3$ + OH reaction, J. Phys. Chem. B 112 (2008) 328–335.
[53] J. Zheng, D.G. Truhlar, Kinetics of hydrogen-transfer isomerizations of butoxyl radicals, Phys. Chem. Chem. Phys. 12 (2010) 7782–7793.
[54] M.J. Kurylo, V.L. Orkin, Determination of atmospheric lifetimes via the measurement of OH radical kinetics, Chem. Rev. 103 (2003) 5049–5076.
[55] Ø. Hodnebrog, M. Etminan, J.S. Fuglestvedt, G. Marston, G. Myhre, C.J. Nielsen, K.P. Shine, T.J. Wallington, Global warming potentials and radiative efficiencies of halocarbons and related compounds: a comprehensive review, Rev. Geophys. 51 (2013) 300–378.